PAPER

Curie temperature study of $Y(Fe_{1-x}Co_x)_2$ and $Zr(Fe_{1-x}Co_x)_2$ systems using mean field theory and Monte Carlo method

View the article online for updates and enhancements.

IOP ebooks™

Bringing together innovative digital publishing with leading authors from the global scientific community.

Start exploring the collection–download the first chapter of every title for free.

Curie temperature study of $Y(Fe_{1-x}Co_x)_2$ and $Zr(Fe_{1-x}Co_x)_2$ systems using mean field theory and Monte Carlo method

Bartosz Wasilewski[1], Wojciech Marciniak[2,3] and Mirosław Werwiński[1]

[1] Institute of Molecular Physics, Polish Academy of Sciences, M. Smoluchowskiego 17, 60-179 Poznań, Poland

[2] Institute of Physics, Faculty of Technical Physics, Poznan University of Technology, Piotrowo 3, 61-138 Poznań, Poland

E-mail: wojciech.ro.marciniak@student.put.poznan.pl

Abstract

Cubic Laves phases including YFe_2, YCo_2, $ZrFe_2$, and $ZrCo_2$ are considered as promising candidates for application in hydrogen storage and magnetic refrigeration. While YFe_2 and $ZrFe_2$ are ferromagnets, alloying with Co decreases magnetic moments and Curie temperatures (T_C) of pseudobinary $Y(Fe_{1-x}Co_x)_2$ and $Zr(Fe_{1-x}Co_x)_2$ systems, leading to the paramagnetic states of YCo_2 and $ZrCo_2$. The following study focuses on the investigation of Curie temperature of the $Y(Fe_{1-x}Co_x)_2$ and $Zr(Fe_{1-x}Co_x)_2$ system from first principles. To do it, Monte Carlo (MC) simulations and the mean field theory (MFT) based on the disordered local moments (DLM) calculations are used. The DLM-MFT results agree qualitatively with the experimental data from the literature and preserve the characteristic features of $T_C(x)$ dependencies for both $Y(Fe_{1-x}Co_x)_2$ and $Zr(Fe_{1-x}Co_x)_2$. However, we have encountered complications in the Co-rich regions due to failure of the local density approximation (LDA) in describing the Co magnetic moment in the DLM state. The analysis of Fe–Fe exchange couplings for YFe_2 and $ZrFe_2$ phases indicates that the nearest-neighbor interactions play the main role in the formation of T_C.

Keywords: Curie temperature, ab initio, Laves phases, Monte Carlo, mean field theory

(Some figures may appear in colour only in the online journal)

1. Introduction

Laves phases are close packed structure intermetallics with a chemical composition AB_2. They are classified into three types: hexagonal $MgZn_2$ (C14), cubic $MgCu_2$ (C15), and hexagonal $MgNi_2$ (C36). In this work we investigate theoretically the C15 cubic phases YFe_2 and $ZrFe_2$ together with their pseudobinary alloys with YCo_2 and $ZrCo_2$. The mentioned systems were recently intensively studied from both fundamental and application points of view. For hydrogen storage applications, the $ZrFe_2$, YFe_2 and its alloys [1–3] together with Zr–Fe–Co [4] and $Zr(Cr_{0.5}Ni_{0.5})_2$ [5] ternary alloys were considered. $ZrFe_2$

and its role in the hydrogen storage behaviour of selected hydride systems has also been discussed [6, 7]. Furthermore, YCo_2 alloys with rare-earth elements $R_{1-x}Y_xCo_2$ (R = Er, Gd) were investigated as magnetocaloric materials for application in magnetic refrigerators [8, 9], similar like $Er_{1-x}Zr_xFe_2$ alloys [10]. The above efforts are supplemented by a number of theoretical studies of mechanical [11], electronic [12], and magnetic properties [13, 14] concerning $ZrFe_2$, YCo_2, and $ZrCo_2$ compounds. The binary XFe_2 and XCo_2 phases (including X = Y, Zr) have been also investigated theoretically from a permanent magnets perspective [15].

One of the key physical quantities of a magnetic material is the Curie temperature (T_C) indicating the magnetic phase transition. It is known from experiment that the YFe_2 and

[3] Author to whom any correspondence should be addressed.

J. Phys. D: Appl. Phys. **51** (2018) 175001

B Wasilewski *et al*

ZrFe$_2$ are ferromagnets with Curie temperatures of 550 and 620 K, respectively [16, 17]. YCo$_2$ is an exchange enhanced Pauli paramagnet and ZrCo$_2$ is a regular Pauli paramagnet [18]. Furthermore, YCo$_2$ undergoes a metamagnetic transition at 70 T and 10 K [19], while ZrCo$_2$ does not exhibit such a transition [20]. In YCo$_2$ magnetic ordering can be also induced by introducing either defects or chemical disorder [21, 22]. Taking into account the recent interest in YFe$_2$, ZrFe$_2$, YCo$_2$, and ZrCo$_2$, we decided to investigate from first principles the T_C of the above compounds and their pseudobinary alloys. We try to explain the dependence of T_C on first neighbor interactions for YFe$_2$ and ZrFe$_2$ and to draw a relation between the T_C and chemical composition. Out of several methods that allow to study the T_C from first principles, we use in this work the mean field theory based on the disordered local moment method (DLM-MFT) and Monte Carlo (MC) method. The MC method allows us to make predictions by simulating the Heisenberg model of a given composition, such as magnetization (M) and susceptibility (χ) versus temperature dependencies [23], while using the DLM-MFT we can calculate only the Curie temperature of a given composition.

2. Calculations' details

The Curie temperature can be estimated with the use of the mean field theory (DLM-MFT) by considering the difference in energy between the DLM and ferromagnetic states [24, 25] according to the following equation:

$$T_C^{\text{DLM}-\text{MFT}} = \frac{2}{3}\frac{E_{\text{DLM}} - E_{\text{FM}}}{k_B \cdot c},\tag{1}$$

for $E_{\text{DLM}} - E_{\text{FM}} > 0$, and

$$T_C^{\text{DLM}-\text{MFT}} = 0,\tag{2}$$

otherwise. The E_{DLM} and E_{FM} are respectively the total energies for the DLM and ferromagnetic states, k_B is the Boltzmann constant, and c is the concentration of magnetic atoms. In this work we use the coherent potential approximation (CPA) [26] in two ways. One way is to treat the chemical disorder (ferromagnetic states) and the other is to treat the magnetic and chemical disorders in the DLM calculations. Here, we simultaneously use both methods. Magnetically disordered state is done by forming a model with half of the magnetic moments pointing one direction and half pointing the opposite. For example, to model the paramagnetic state of Zr(Fe$_{0.5}$Co$_{0.5}$)$_2$ we create a following configuration Zr(Fe$_{0.25\uparrow}$Fe$_{0.25\downarrow}$Co$_{0.25\uparrow}$Co$_{0.25\downarrow}$)$_2$. The arrows indicate the direction of the magnetic moment on each atom. The magnetic moment on Zr is of induced character and there was no need to treat it with the DLM.

The second method used in this work to determine the Curie temperature is MC simulations. The classical (i.e. not quantum) MC simulations were done using the Uppsala atomistic spin dynamics (UppASD) code [27] with the magnetic moments and exchange integrals obtained from the spin polarized relativistic Korringa–Kohn–Rostoker (SPR-KKR) [28, 29] calculations. The exchange integrals were calculated

Table 1. Atomic coordinates for Y(Fe$_{1-x}$Co$_x$)$_2$ and Zr(Fe$_{1-x}$Co$_x$)$_2$, space group *Fd-3m* (no. 227), origin choice two.

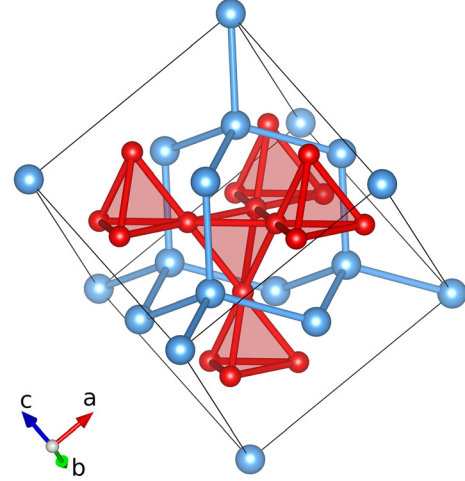| Atom	Site	x	y	z
Y/Zr	8a	1/8	1/8	1/8
Fe/Co	16d	1/2	1/2	1/2

Figure 1. Crystal structure of the cubic MgCu$_2$-type Laves phase. The large blue balls represent Mg atoms and the small red balls indicate Cu atoms.

using the method of Liechtenstein *et al* [30] with respect to the ferromagnetic state. In the MC simulations we determine T_C from the position of the peak in the temperature dependence of susceptibility. The radius of the exchange integrals cutoff sphere in the Heisenberg model was set up to 1.5 lattice parameter (a) which means that only the atomic pairs separated by distance below 1.5 a were considered. The simulated system consisted of 8800 atoms with periodic boundary conditions. The simulations have been checked for convergence with the radius of the Heisenberg model cutoff sphere. In this work, the DLM calculations were performed for the whole range of Co concentrations, while the MC simulations were limited to YFe$_2$ and ZrFe$_2$.

The occupied atomic position and the space group of the C15 cubic Laves phase can be found in table 1. The unit cell is presented in figure 1, which was created with the use of the VESTA code [31]. For the calculations of the binary compositions we used the experimental values of the lattice parameters which are equal to 7.36 [17], 7.22 [17], 7.07 [32], and 6.96 [32] Å for YFe$_2$, YCo$_2$, ZrFe$_2$, and ZrCo$_2$ respectively. Since in the experiment the lattice parameters of Y(Fe$_{1-x}$Co$_x$)$_2$ and Zr(Fe$_{1-x}$Co$_x$)$_2$ change almost linearly with Co concentration [17, 32], for the intermediate composition we assumed linear behavior of the lattice parameters. The electronic band structure calculations for the whole concentration range of Y(Fe$_{1-x}$Co$_x$)$_2$ and Zr(Fe$_{1-x}$Co$_x$)$_2$ systems were performed using the full-potential local-orbital minimum-basis scheme FPLO5.00 [33, 34]. The chemical and magnetic disorder on the Fe/Co site was modeled with the CPA. Due to limitations of FPLO5.00, we used the scalar-relativistic approach
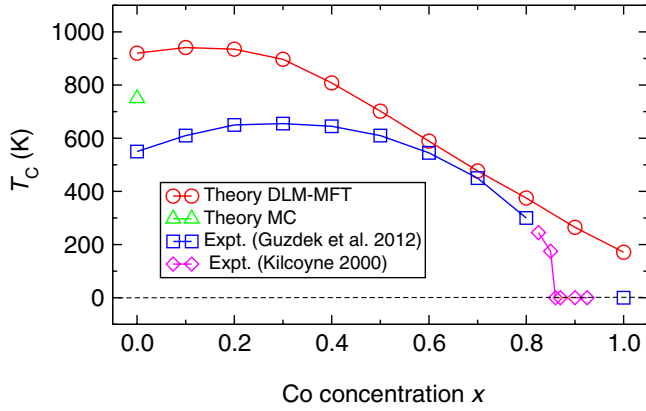
Figure 2. Curie temperatures of $Y(Fe_{1-x}Co_x)_2$ as calculated with the DLM-MFT and MC methods compared with experimental data from works of Guzdek *et al* [17] and Kilcoyne [37].

Table 2. Curie temperatures (in K) of the YFe_2, YCo_2, $ZrFe_2$, and $ZrCo_2$ as calculated with the DLM-MFT and MC methods in comparison with the experimental results from literature [16, 17].

	YFe_2	YCo_2	$ZrFe_2$	$ZrCo_2$
DLM-MFT	920	171	846	0
MC	750	—	780	—
Expt.	550	0	620	0

and local density approximation in the form of Perdew and Wang (PW92) [35]. The basis was optimized. The $3s3p$ Fe/Co orbitals were treated as semicore and $4s4p3d$ as valence. The Y and Zr $4s4p$ orbitals were treated as semicore and $5s5p4d$ as valence. After convergence tests we have chosen a $12 \times 12 \times 12$ **k**-mesh. We applied simultaneous energy and charge density convergence criteria of $\sim 2.72 \times 10^{-7}$ eV (10^{-8} Ha) and 10^{-6}, respectively.

The MC simulations were performed using magnetic moments and exchange couplings obtained with the version 7.6 of the SPR-KKR code. The calculations were performed using 40 energy points on a semicircular energy path and 1000 irreducible **k**-points, corresponding to a $36 \times 36 \times 36$ mesh. For the exchange-correlation potential we employed the Vosko–Wilk–Nusair (VWN) [36] form of the local density approximation (LDA). The SPR-KKR calculations were done in the full relativistic and full potential approaches.

3. Results and discussion

3.1. $Y(Fe_{1-x}Co_x)_2$

In figure 2, we present our computational results for the Curie temperatures of the $Y(Fe_{1-x}Co_x)_2$ system compared with the experiment. Table 2 summarizes the results for the boundary binary compounds.

For the $Y(Fe_{1-x}Co_x)_2$ system, our calculations show qualitative agreement with the experiment for the concentration range $x \leqslant 0.8$ and preserve the characteristic Slater–Pauling-like maximum. A similar maximum also appears in the total magnetic moment versus Co concentration graph (not shown). The magnetic moments on Fe obtained with SPR-KKR, which

Table 3. Magnetic moments (in μ_B) for $ZrFe_2$ and YFe_2, as used in UppASD MC simulations compared with the experimental results from literature [18]. Magnetic moments *per Fe* include opposite contributions from $4d$ elements and are equal to half of the total magnetic moment per formula unit, while the calculated magnetic moments *on Fe* should be added together with the opposite $4d$ shares to get the total magnetic moment.

	YFe_2	$ZrFe_2$
On Fe (theory)	1.85	1.78
Per Fe (theory)	1.66	1.58
Per Fe (expt.)	1.49	1.51

are in good agreement with the experiment, are listed in table 3. The Curie temperatures on the Fe-rich side calculated with the DLM-MFT are however significantly overestimated relative to the experimental values. Similar disagreement between the critical temperatures measured and calculated with the mean field approximation has been found for other systems before and it was considered as a characteristic behavior of the mean field method [29, 38, 39]. The overestimation of T_C originates from the fact that the mean field approximation neglects the spin fluctuations which makes the magnetic moments more rigid [40]. On the Co-rich side, the predicted ferromagnetic ground state of YCo_2 is wrong. The comparison of non-magnetic and ferromagnetic states of YCo_2 calculated in LDA at experimental lattice constants leads to an incorrect magnetic ground state [41]. Furthermore, we observe that the formation of DLM state of YCo_2 fails as the initially opposite magnetic moments on Co collapse to zero (non-magnetic state) after the convergence. The problem with an accurate description of the magnetic state of Co alloys has been addressed previously by Edströem *et al* [42]. They have related the difficulties to an insufficient treatment of correlation effects in LDA/GGA, which can be overcome by application of the dynamical mean field theory (DMFT) [43]. For YCo_2 we have made additional LDA + U calculations, with the corrections applied to Co $3d$ orbitals. However we have finished once again with a collapse of Co moments in the DLM state. A failure of the LDA + U approach suggests the need for dynamical correlations in this case. In a similar collapse of magnetic moments on Co, as observed for YCo_2, we found for all DLM states of the considered $Y(Fe_{1-x}Co_x)_2$ phases. The overestimation of T_C in MFT on one hand and the insufficient treatment of correlation effects in LDA on the other are the reasons why the calculated T_C versus Co concentration dependence does not exhibit a ferromagnet-paramagnet phase transition. The evolution of Curie temperature with Co concentration is correlated with evolution of an electronic structure of the material. To give a feeling of what is happening as more Co atoms replace Fe ones in figure 3, we present the total densities of states (DOS) for several Co concentrations. The YFe_2 ($x = 0$) valence band consists mainly of Fe $3d$ states. The DOS of YFe_2 is strongly spin polarized and the most important contributions lay above -4 eV. When alloying Co ($Z = 27$) for Fe ($Z = 26$) to the system. Additional electrons are delivered, filling the valence band. With the increase of Co concentration, the less occupied spin channel is filling leading to a decrease of spin polarization.
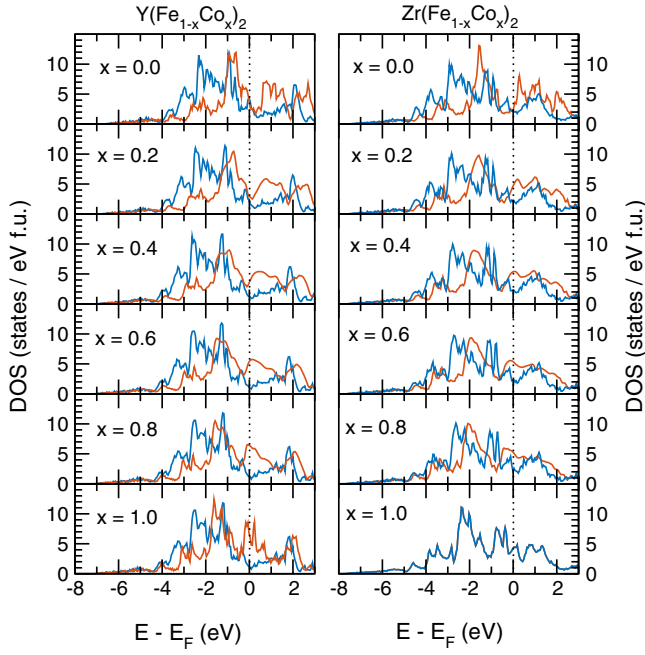
J. Phys. D: Appl. Phys. 51 (2018) 175001

B Wasilewski *et al*

Figure 3. The densities of states (DOS) of $Y(Fe_{1-x}Co_x)_2$ and $Zr(Fe_{1-x}Co_x)_2$ as calculated with the FPLO5-LDA-CPA method. Red and blue colors represent two spin channels.
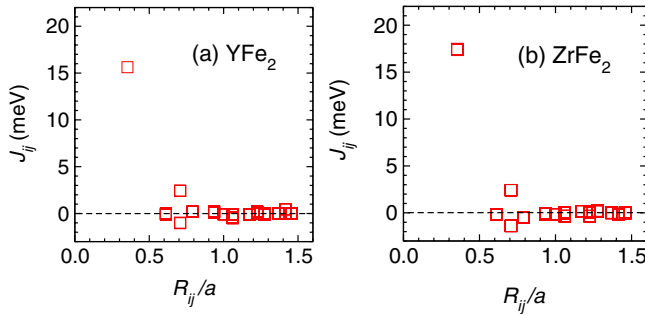

Figure 4. The Fe–Fe exchange couplings versus normalized distance for (a) YFe_2 and (b) $ZrFe_2$ as calculated with the FP-SPR-KKR.

The magnetic moments on the Y/Zr atoms are of induced character and are expected to vanish with temperature, therefore we left them out of the simulated Heisenberg model. By looking at the graph of exchange interactions for YFe_2, see figure 4(a), we can see that the dominant exchange coupling is positive, as expected for a ferromagnet. Besides direct exchange there can be also observed interactions of oscillatory character. As for the MC simulations for the YFe_2, see figure 5, the agreement with the experiment is reasonable where experimental $T_C = 550$ K and our simulations yield a value of $T_C = 750$ K. We can also see that the $M(T)$ curve has a Curie–Weiss character, as expected.

3.2. $Zr(Fe_{1-x}Co_x)_2$

For the $Zr(Fe_{1-x}Co_x)_2$ system, there is qualitative agreement of the calculated Curie temperatures with the experimental dependence, see figure 6. The experiment has an almost linear course with x, ranging from $T_C = 620$ K [16] at $x = 0$ to 0 K
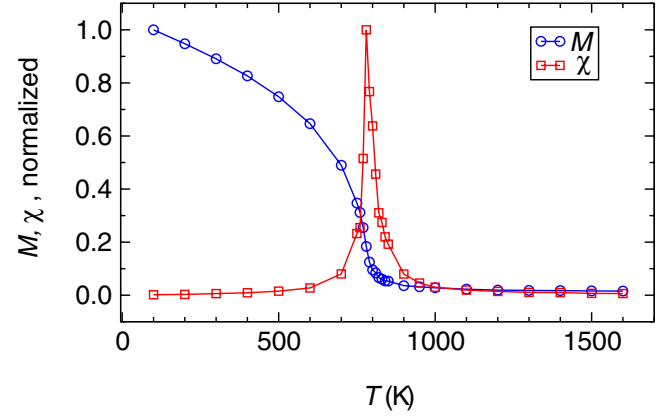

Figure 5. The normalized magnetization and susceptibility temperature dependencies for YFe_2 as calculated by MC simulations with the UppASD code with parameters from the FP-SPR-KKR.
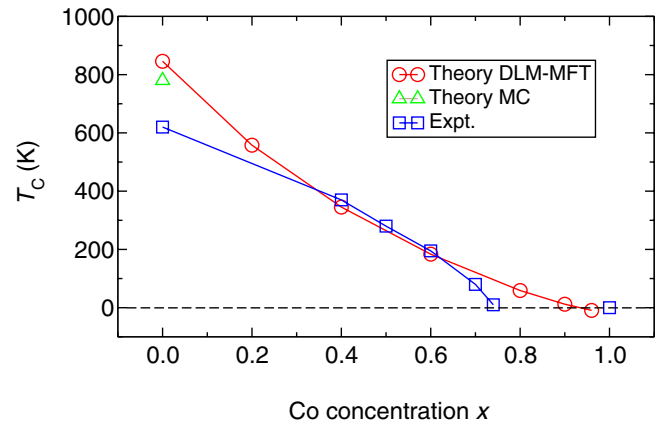

Figure 6. Curie temperatures of $Zr(Fe_{1-x}Co_x)_2$ as calculated with the DLM-MFT and MC methods in comparison with experimental data from literature [16].

at $x \sim 0.75$, while our theoretical results also show that T_C is decreasing with x and equal zero for $x \sim 0.95$. The discrepancy with the experiment in the Co-rich region can be explained similarly as before for $Y(Fe_{1-x}Co_x)_2$. Furthermore, figure 3 presents DOSs for several Co concentrations. As Zr has one more electron than Y, the presented valence bands of $Zr(Fe_{1-x}Co_x)_2$ alloys are slightly more filled than of corresponding $Y(Fe_{1-x}Co_x)_2$ alloys. The observed, for $Zr(Fe_{1-x}Co_x)_2$ system, decrease of T_C with x is correlated with a decrease of spin splitting in DOS induced by band filling. In agreement with experiment, we do not observe ferromagnetic ground state for $ZrCo_2$.

For the $ZrFe_2$ the nearest neighbor Fe–Fe exchange coupling is positive and dominant. Similarly to YFe_2, $ZrFe_2$ exchange couplings also have oscillatory character, see figure 4(b). The $ZrFe_2$ magnetization and susceptibility MC simulations, see figure 7, predict a ferromagnetic state for $ZrFe_2$ with the Curie temperature of ~ 780 K which is in a reasonable agreement with the experimental value of 620 K. Interestingly for the $ZrFe_2$ the MC simulations with the dominant exchange coupling only yielded $T_C \sim 550$ K (230 K lower than for exchange couplings considered up

J. Phys. D: Appl. Phys. 51 (2018) 175001
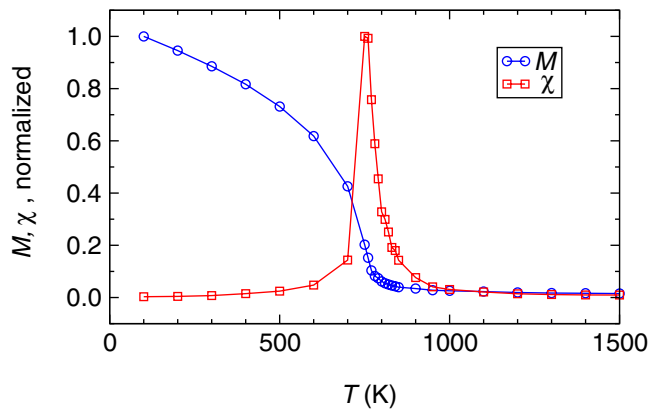
B Wasilewski *et al*

Figure 7. The normalized magnetization and susceptibility temperature dependencies for ZrFe$_2$ as calculated by MC simulations with the UppASD code with parameters from the FP-SPR-KKR.

to 1.5 *a*) which shows how the system is sensitive to small contributions in relatively large numbers and the importance of checking for convergence with the radius of the exchange integrals cutoff sphere. Analogously to YFe$_2$, the ZrFe$_2$ $M(T)$ curve also has a Curie–Weiss character. We have decided not to model YCo$_2$ and ZrCo$_2$ with MC simulations due to the fact that the exchange couplings and magnetic moments used in the mentioned calculations were obtained with respect to the ferromagnetic ground state and YCo$_2$ and ZrCo$_2$ are Pauli paramagnets.

4. Summary and conclusions

The Curie temperatures of $Y(Fe_{1-x}Co_x)_2$ and $Zr(Fe_{1-x}Co_x)_2$ systems were calculated *ab initio* based on the disordered local moment method within the mean field theory (DLM-MFT). Furthermore, the Curie temperatures of YFe$_2$ and ZrFe$_2$ were calculated by Monte Carlo (MC) simulations. Comparing the results of our calculations with experimental data from literature, a good qualitative agreement is observed. The main features of experimental $T_C(x)$ plots are reproduced, however with some limitations. Both approaches, the DLM-MFT and MC tend to overestimate the T_C with the most troublesome region on the Co-rich side, where the systems undergo a ferromagnetic-paramagnetic phase transition. For $Y(Fe_{1-x}Co_x)_2$ the DLM-MFT approach correctly predicts the characteristic maximum in T_C for intermediate compositions but fails by predicting the ferromagnetic ground state of the YCo$_2$ paramagnet. For $Zr(Fe_{1-x}Co_x)_2$ the DLM-MFT predicts both the monotonic decrease of T_C with x and the critical Co concentration above which the system becomes paramagnetic. However, the exact value of the critical concentration is overestimated. The MC simulations for YFe$_2$ and ZrFe$_2$ indicate that the nearest neighbors Fe–Fe exchange interactions are the most responsible for the value of T_C. From the point of view of computations, this paper shows that the accurate T_C analysis for alloys is feasible with coherent potential approximation used for simulation of the magnetically disordered DLM state.

ORCID iDs

Wojciech Marciniak https://orcid.org/0000-0002-9173-5496
Mirosław Werwiński https://orcid.org/0000-0003-1934-4818

References

[1] Wiesinger G, Paul-Boncour V, Filipek S M, Reichl C, Marchuk I and Percheron-Guégan A 2005 *J. Phys.: Condens. Matter* **17** 893
[2] Isnard O, Paul-Boncour V, Arnold Z, Colin C V, Leblond T, Kamarad J and Sugiura H 2011 *Phys. Rev.* B **84** 094429
[3] Li Z, Wang H, Ouyang L, Liu J and Zhu M 2016 *J. Alloys Compd.* **689** 843
[4] Jat R A, Singh R, Parida S C, Das A, Agarwal R, Mukerjee S K and Ramakumar K L 2015 *Int. J. Hydrog. Energy* **40** 5135
[5] Merlino A R, Luna C R, Juan A and Pronsato M E 2016 *Int. J. Hydrog. Energy* **41** 2700
[6] Shahi R R, Bhatanagar A, Pandey S K, Shukla V, Yadav T P, Shaz M A and Srivastava O N 2015 *Int. J. Hydrog. Energy* **40** 11506
[7] Shukla V, Bhatnagar A, Soni P K, Vishwakarma A K, Shaz M A, Yadav T P and Srivastava O N 2017 *Phys. Chem. Chem. Phys.* **19** 9444
[8] Baranov N V, Proshkin A V, Czternasty C, Meißner M, Podlesnyak A and Podgornykh S M 2009 *Phys. Rev.* B **79** 184420
[9] Pierunek N, Śniadecki Z, Werwiński M, Wasilewski B, Franco V and Idzikowski B 2017 *J. Alloys Compd.* **702** 258
[10] Mican S, Benea D, Mankovsky S, Polesya S, Gînscă O and Tetean R 2013 *J. Phys.: Condens. Matter* **25** 466003
[11] Chen S, Sun Y, Duan Y H, Huang B and Peng M J 2015 *J. Alloys Compd.* **630** 202
[12] Bhatt S, Kumar K, Arora G, Bapna K and Ahuja B L 2016 *Radiat. Phys. Chem.* **125** 109
[13] Zhang W and Zhang W 2015 *J. Appl. Phys.* **117** 163917
[14] Zhuravleva I P, Grechnev G E, Panfilov A S and Lyogenkaya A A 2017 *Low Temp. Phys.* **43** 597
[15] Kumar P, Kashyap A, Balamurugan B, Shield J E, Sellmyer D J and Skomski R 2014 *J. Phys.: Condens. Matter* **26** 064209
[16] Hilscher G and Gmelin E 1978 *J. Phys. Colloques* **39** C6
[17] Guzdek P, Pszczoła J, Chmist J, Stoch P, Stoch A and Suwalski J 2012 *J. Alloys Compd.* **520** 72
[18] Yamada Y and Ohmae H 1980 *J. Phys. Soc. Japan* **48** 1513
[19] Goto T, Sakakibara T, Murata K, Komatsu H and Fukamichi K 1990 *J. Magn. Magn. Mater.* **90** 700
[20] Yamada H and Shimizu M 1990 *J. Magn. Magn. Mater.* **90** 703
[21] Śniadecki Z, Werwiński M, Szajek A, Rößler U K and Idzikowski B 2014 *J. Appl. Phys.* **115** 17E129
[22] Śniadecki Z, Kopcewicz M, Pierunek N and Idzikowski B 2015 *Appl. Phys.* A **118** 1273

J. Phys. D: Appl. Phys. **51** (2018) 175001

B Wasilewski *et al*

[23] Eriksson O, Bergman A, Bergqvist L and Hellsvik J 2017 *Atomistic Spin Dynamics: Foundations and Applications* (Oxford: Oxford University Press)

[24] Gyorffy B L, Pindor A J, Staunton J, Stocks G M and Winter H 1985 *J. Phys. F: Met. Phys.* **15** 1337

[25] Bergqvist L and Dederichs P H 2007 *J. Phys.: Condens. Matter* **19** 216220

[26] Soven P 1967 *Phys. Rev.* **156** 809

[27] Skubic B, Hellsvik J, Nordström L and Eriksson O 2008 *J. Phys.: Condens. Matter* **20** 315203

[28] Ebert H *et al* The Munich SPR-KKR Package, Version 7.6 http://ebert.cup.uni-muenchen.de/SPRKKR

[29] Ebert H, Ködderitzsch D and Minár J 2011 *Rep. Prog. Phys.* **74** 096501

[30] Liechtenstein A I, Katsnelson M I and Gubanov V A 1984 *J. Phys. F: Met. Phys.* **14** L125

[31] Momma K and Izumi F 2011 *J. Appl. Crystallogr.* **44** 1272

[32] Muraoka Y, Shiga M and Nakamura Y 1979 *J. Phys. F: Met. Phys.* **9** 1889

[33] Koepernik K, Velický B, Hayn R and Eschrig H 1997 *Phys. Rev. B* **55** 5717

[34] Koepernik K and Eschrig H 1999 *Phys. Rev. B* **59** 1743

[35] Perdew J P and Wang Y 1992 *Phys. Rev. B* **45** 13244

[36] Vosko S H, Wilk L and Nusair M 1980 *Can. J. Phys.* **58** 1200

[37] Kilcoyne S H 2000 *Physica B* **276–8** 660

[38] Ke L, Belashchenko K D, van Schilfgaarde M, Kotani T and Antropov V P 2013 *Phys. Rev. B* **88** 024404

[39] Hedlund D, Cedervall J, Edström A, Werwiński M, Kontos S, Eriksson O, Rusz J, Svedlindh P, Sahlberg M and Gunnarsson K 2017 *Phys. Rev. B* **96** 094433

[40] Rusz J, Bergqvist L, Kudrnovský J and Turek I 2006 *Phys. Rev. B* **73** 214412

[41] Khmelevskyi S, Mohn P, Redinger J and Weinert M 2005 *Phys. Rev. Lett.* **94** 146403

[42] Edström A *et al* 2015 *Phys. Rev. B* **92** 174413

[43] Kotliar G, Savrasov S Y, Haule K, Oudovenko V S, Parcollet O and Marianetti C A 2006 *Rev. Mod. Phys.* **78** 865